

# Supplement to *Aging and Source-Dependent Volatility of Organic Aerosols in Seoul: Revisiting the Oxidation–Volatility Link*

Hwajin Kim<sup>1,2,\*</sup>, Jiwoo Jeong<sup>1</sup>, Jihye Moon<sup>1</sup>, Hyun Gu Kang<sup>2,3</sup>

<sup>1</sup>Department of Environmental Health Sciences, Graduate School of Public Health, Seoul National University, 08826 Seoul, South Korea

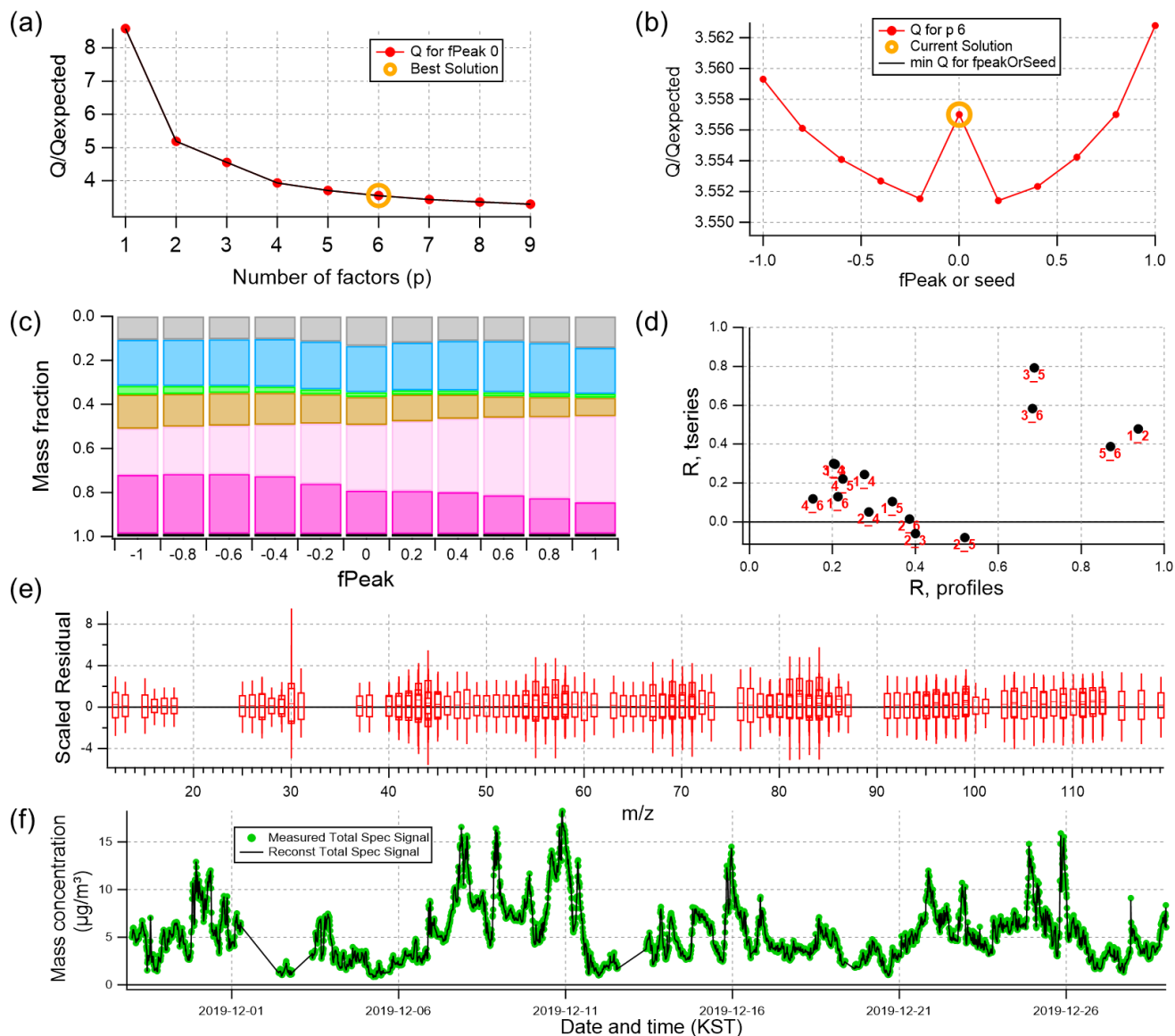
<sup>2</sup>Institute of Health and Environment, Graduate School of Public Health, Seoul National University, 08826 Seoul, South Korea

<sup>3</sup>Now at Multiphase Chemistry Department, Max Planck Institute for Chemistry, 55128 Mainz, Germany

Correspondence to: Hwajin Kim (khj0116@snu.ac.kr)

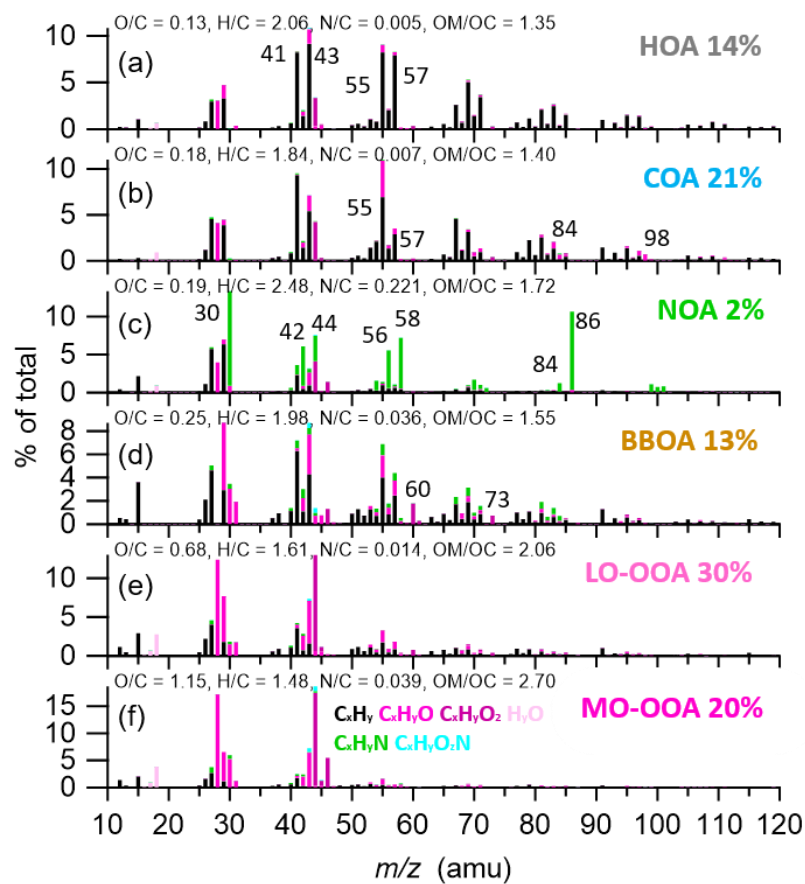
**Table S1.** Vaporization enthalpy ( $\Delta H_{\text{exp}}$ ) and mass accommodation coefficient ( $\alpha_m$ ) values of each factor resolved by PMF.

PMF factor	Vaporization enthalpy ( $\Delta H_{\text{exp}}$ , kJ mol <sup>-1</sup> ) ( $40 \leq \Delta H_{\text{exp}} \leq 200$ )	Mass accommodation coefficient ( $\alpha_m$ ) ( $0.1 \leq \alpha_m \leq 1$ )
HOA	165.86	0.81
COA	161.65	0.79
NOA	167.08	0.82
BBOA	163.84	0.80
LO-OOA	151.57	0.80
MO-OOA	165.00	0.79

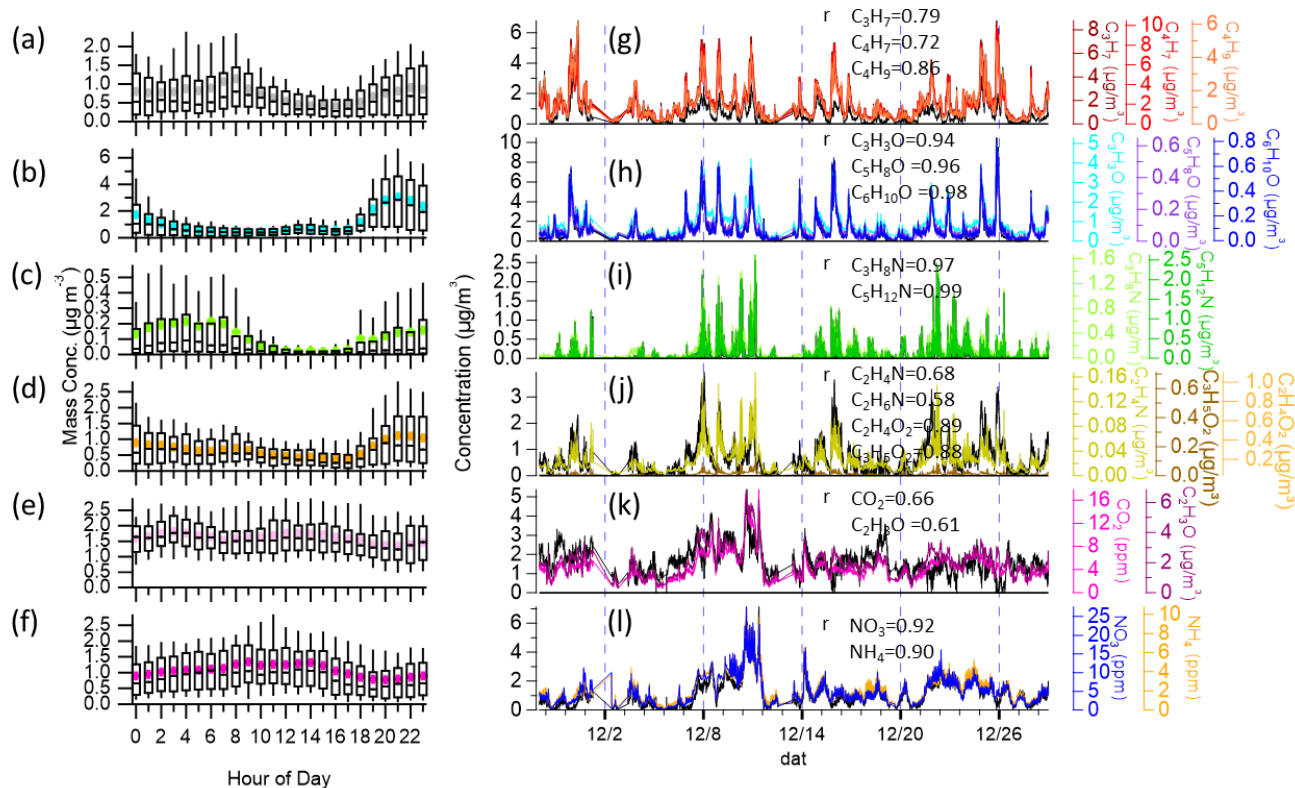


16

17 **Figure S1.** Key diagnostic plots for the six-factor solution resolved by PMF analysis: (a)  $Q/Q_{exp}$  against the number of factors  
 18 ( $p$ ), (b)  $Q/Q_{exp}$  as a function of fPeak, (c) mass fractional contribution of each PMF factor to the total mass, (d) Pearson's  $r$   
 19 correlation coefficients for correlations among the time series and mass spectra of factors, (e) box and whiskers plot showing  
 20 the distributions of the scaled residuals for each  $m/z$ , (f) time series of the measured mass and the reconstructed mass from the  
 21 sum of the 6 factors.



23 **Figure S2.** High-resolution mass spectra of (a) HOA, (b) COA, (c) NOA, (d) BBOA, (e) LO-OOA, and MO-OOA resolved  
24 by PMF analysis.



25

26 **Figure S3.** Diurnal variations of (a) HOA, (b) COA, (c) NOA, (d) BBOA, (e) LO-OOA, and (f) MO-OOA resolved by PMF  
 27 analysis. Comparison of time series and correlations between OA factors (g) HOA, (h) COA, (i) NOA, (j) BBOA, (k) LO-  
 28 OOA, and (l) MO-OOA and their tracers.

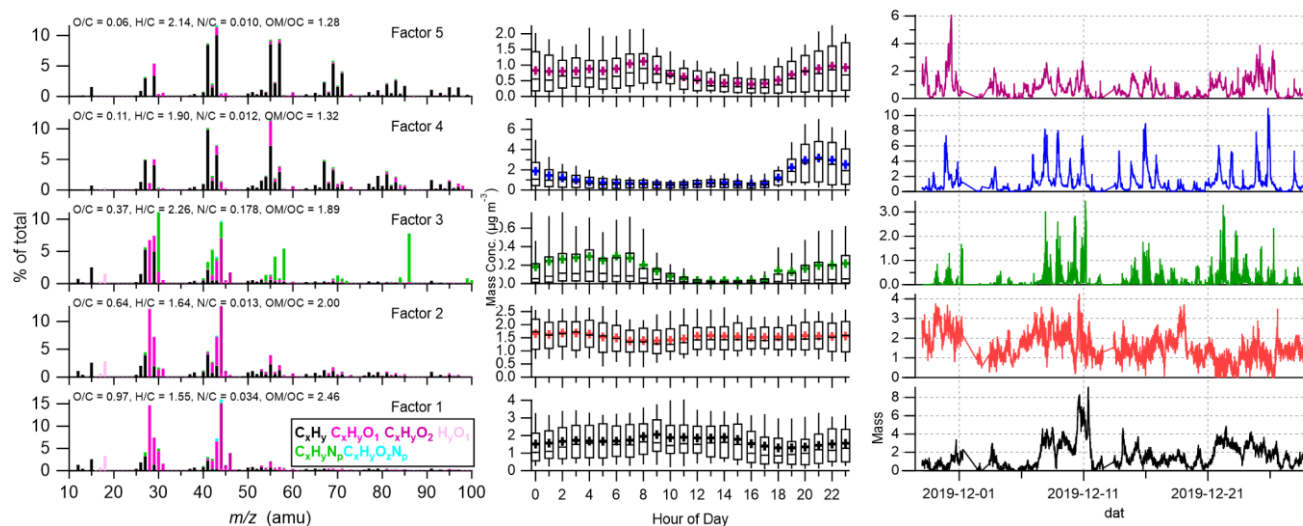


**Figure S4.** 5-factors result from PMF analysis. The five factors from 1 to 5 are HOA, COA, NOA, LO-OOA, and MO-OOA, respectively.

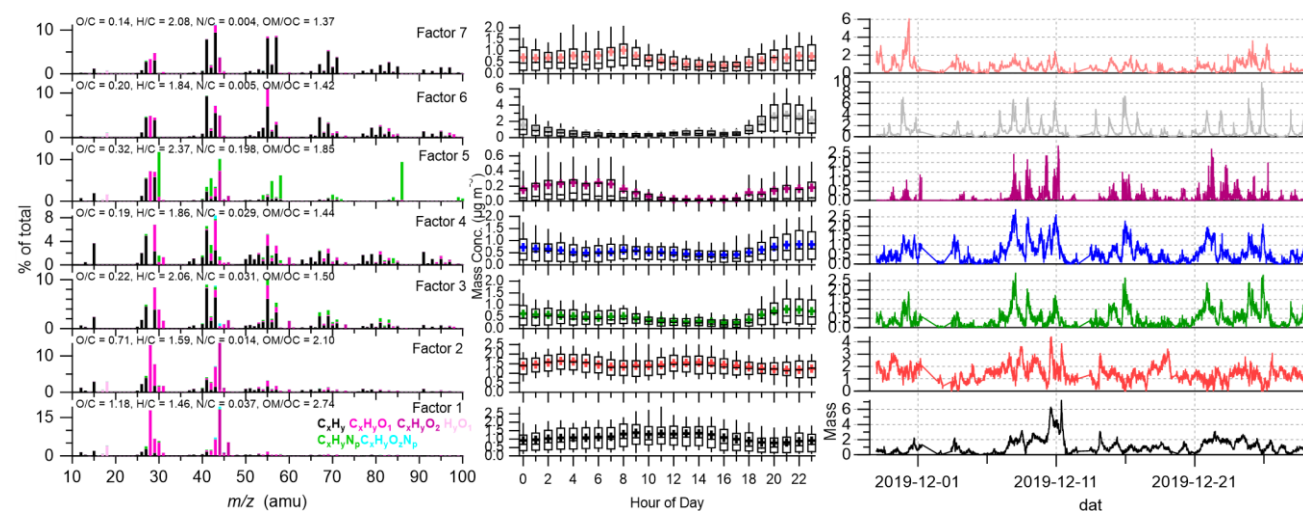


**Figure S5.** 7-factors result from PMF analysis. The five factors from 1 to 7 are HOA, COA, NOA, BBOA1, BBOA2, LO-OOA and MO-OOA, respectively.

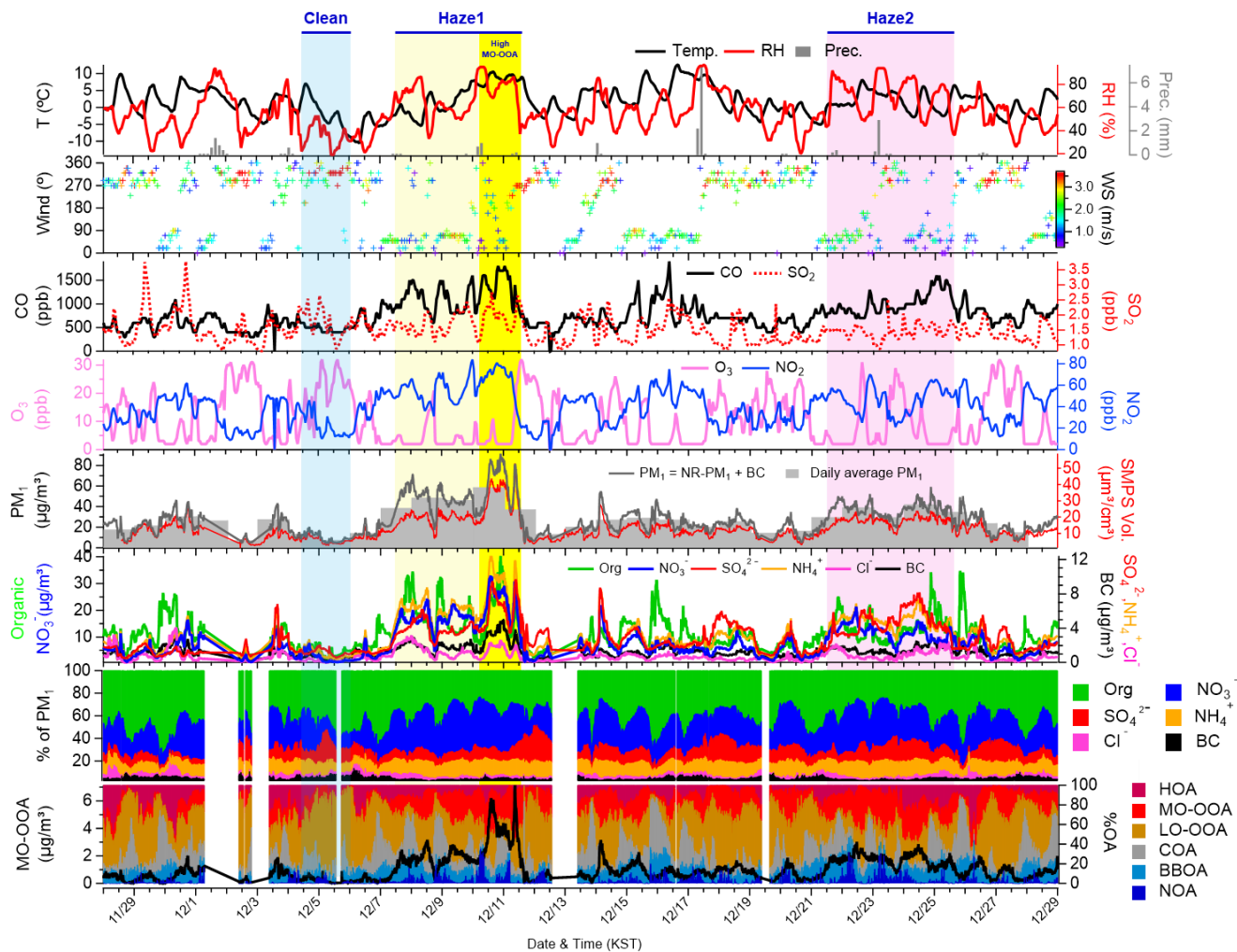
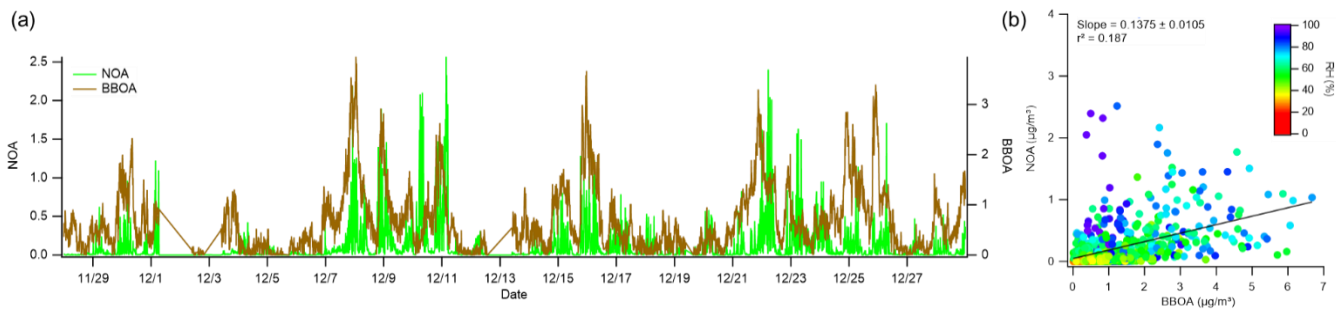
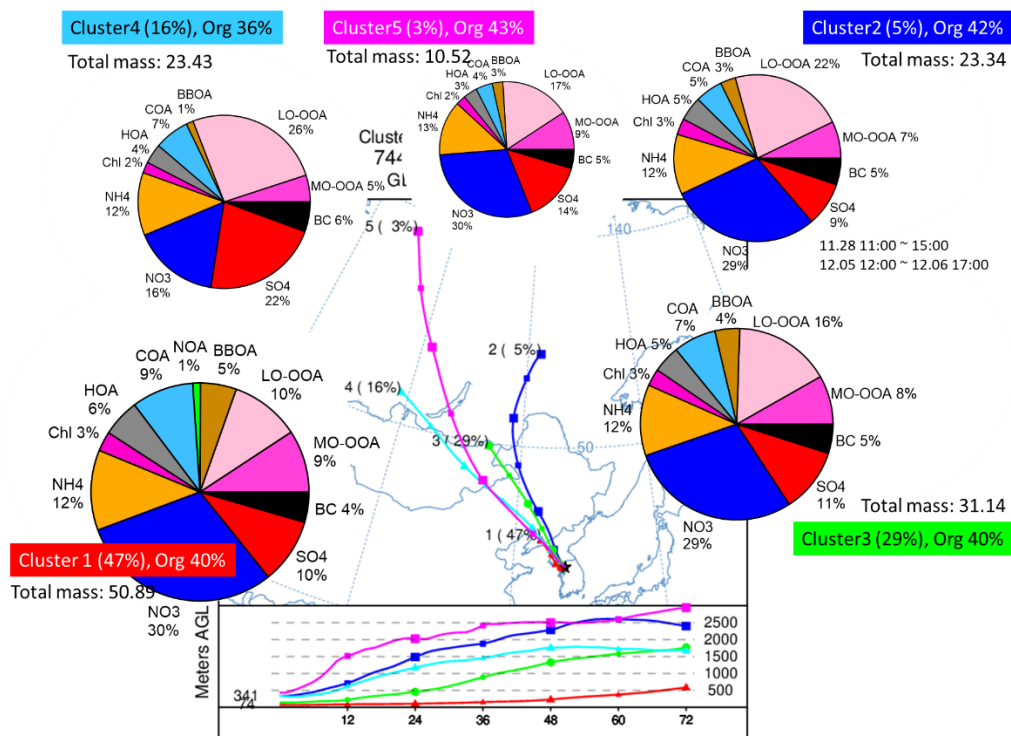


**Figure S6.** Summary of temporal variations of meteorological variables (Temperature, RH, precipitation, wind direction, and wind speed), gaseous pollutants (CO, SO<sub>2</sub>, O<sub>3</sub>, and NO<sub>2</sub>), PM<sub>1</sub>, volume concentration from SMPS, NR-species with BC, mass fractional contribution of NR-species with BC and OA, and concentration of MO-OOA. Blue shade indicates a clean period, whereas yellow and pink shades indicate haze periods. The high MO-OOA period is shaded in bright yellow.



45

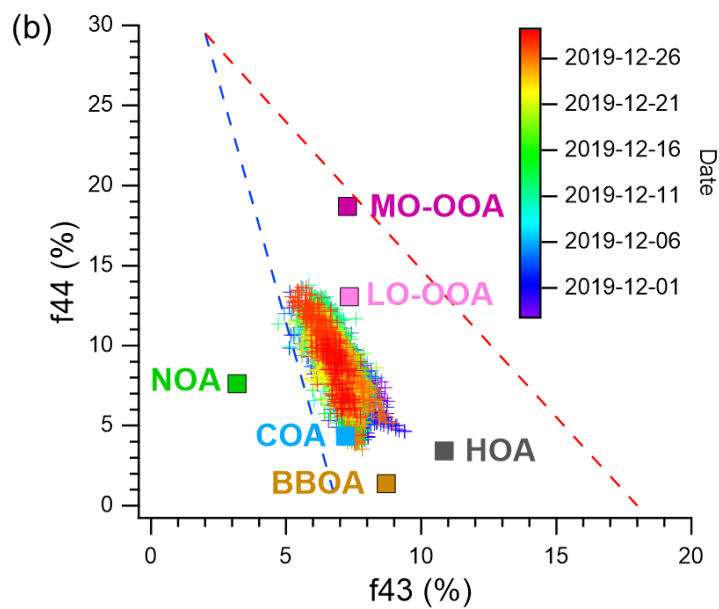
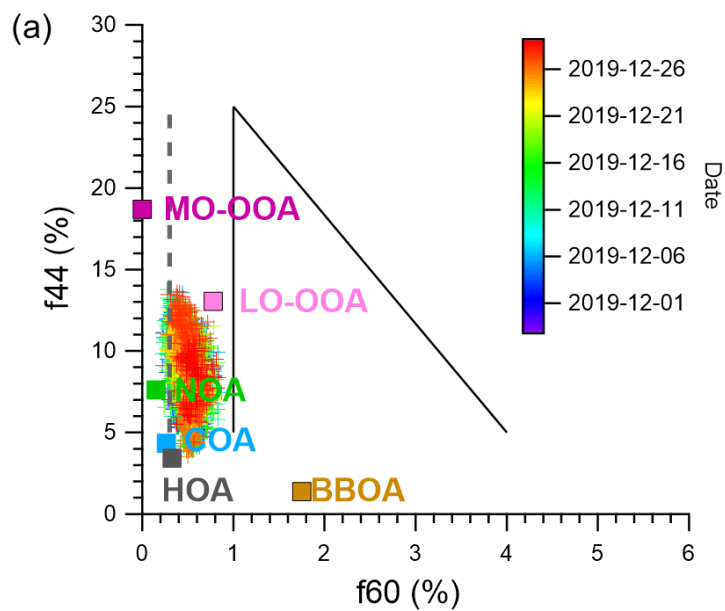
46 **Figure S7.** (a) Time series of NOA and BBOA. (b) Scatter plot showing the correlation and slope between NOA and BBOA.



47  
48  
49

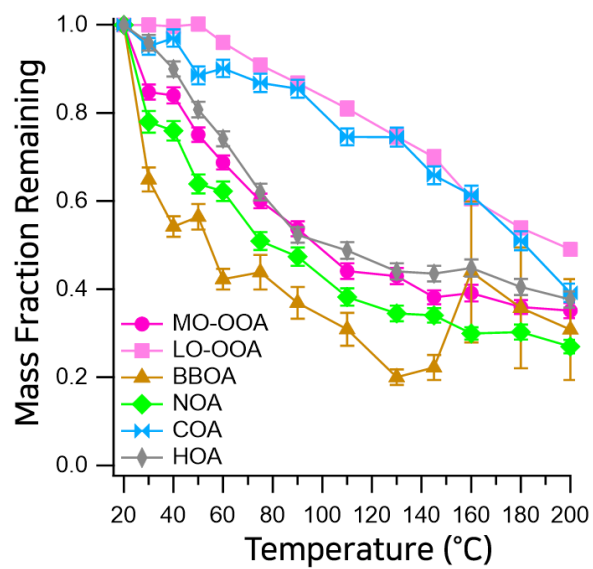
50 **Figure S8.** Back trajectories spanning 96 hours were computed hourly using the Hybrid Single-Particle Lagrangian Integrated  
51 Trajectory (HYSPLIT; ver 5.0.0b). These trajectories originated from release points set at half of the mixing height at the KIST  
52 location (latitude: 37.60° N, longitude: 127.05° E), and on average, the trajectories arrived at an altitude of approximately 191  
53 m (Kim et al., 2017). To discern pollutant properties associated with distinct transport patterns, cluster analysis was conducted  
54 on the trajectories using HYSPLIT4 software. Five clusters of trajectories were identified based on their spatial distribution  
55 similarities. Five clustered back trajectories; Cluster 1 (47%, total mass: 50.89  $\mu\text{g m}^{-3}$ ) from the local area, cluster 2 (5%, total  
56 mass: 23.34  $\mu\text{g m}^{-3}$ ) from northeast, cluster 3 & 4 (29%, total mass: 31.14  $\mu\text{g m}^{-3}$  & 16%, 23.34  $\mu\text{g m}^{-3}$ ) passed through  
57 Mongolia and China, and cluster 5 (3%, total mass: 10.52  $\mu\text{g m}^{-3}$ ) long-range transfer started from Russia.





58

59 **Figure S9.** Scatterplots of (a)  $f_{44}$  ( $\text{CO}_2^+$ ) vs  $f_{60}$  ( $\text{C}_2\text{H}_4\text{O}_2^+$ ), and (b)  $f_{44}$  ( $\text{CO}_2^+$ ) vs  $f_{43}$  ( $\text{C}_2\text{H}_3\text{O}^+$ ).



61 **Figure S10.** Mass fraction remaining (MFR) of 6 different OA factors resolved by PMF analysis.

62   **References**

- 63   Kim, H., Zhang, Q., Bae, G.-N., Kim, J.Y., Lee, S.B., 2017. Sources and atmospheric processing of winter aerosols in Seoul,  
64       Korea: Insights from real-time measurements using a high-resolution aerosol mass spectrometer. *Atmos. Chem. Phys.* 17,  
65       2009–2033. <https://doi.org/10.5194/acp-17-2009-2017>  
66